Materials Today Chemistry 27 (2023) 101355

Contents lists available at ScienceDirect

Materials Today Chemistry

journal homepage: www.journals.elsevier.com/materials-today-chemistry/

3D printing of a palladium-alumina cermet monolithic catalyst: catalytic evaluation in microwave-assisted cross-coupling reactions

C.R. Tubio [a, b], C. Malatini [f], V.L. Barrio [c], C.F. Masaguer [f], M. Amorín [f], W. Nabgan [d], P. Taboada [e], F. Guitián [a], A. Gil [a, **], A. Coelho [a, f, *]

[a] Instituto de Materiales (IMATIUS), Universidade de Santiago de Compostela, 15782, Santiago de Compostela, Spain
[b] BCMaterials, Basque Center for Materials, Applications and Nanostructures, UPV/EHU, Science Park, 48940 Leioa, Spain
[c] School of Engineering (UPV/EHU), Plaza Ingeniero Torres Quevedo 1, 48013 Bilbao, Spain
[d] Departament D'Enginyeria Química, Universitat Rovira I Virgili, Av Països Catalans 26, 43007, Tarragona, Spain
[e] Departamento de Física de La Materia Condensada, Facultad de Física, Universidad de Santiago de Compostela, Santiago de Compostela CP. 15782, Spain
[f] Departamento de Química Orgánica, Facultad de Farmacia, Universidade de Santiago de Compostela, 15782, Santiago de Compostela, Spain

ARTICLE INFO

Article history:
Received 25 July 2022
Received in revised form
23 November 2022
Accepted 6 December 2022
Available online 3 January 2023

Keywords:
3D-printing
Heterogeneous catalyst
Palladium-cross-coupling reactions
Microwave-assisted reactions
Metal-ceramic

ABSTRACT

A straightforward manufacture strategy is proposed to obtain an efficient and robust palladium-alumina (Pd^0/Al_2O_3) cermet monolithic catalyst, specifically designed to perform safe microwave assisted organic synthesis (MAOS). In this approach, a cermet catalyst with high surface area, controlled composition and adapted shape and dimensions to a microwave reactor vessel is generated via 3D printing technology and sintering. The resulting catalyst has been explored in heterogeneous Suzuki, Sonogashira, Stille and Heck cross-coupling reactions, in MAOS. The Pd^0 catalyst is permanently active, stable, without leaching and can be recycled and reused at least 200 reaction cycles. The generation of hot spots, sparking or hazardous discharges is controlled by the effective immobilization of the palladium in the monolithic structure during the reaction. The palladium content is forming part of both the internal and external structure, providing greater mechanical resistance and catalytic activity with respect to the basic ceramic material (alumina).

1. Introduction

Palladium-catalyzed cross-coupling reactions (PCCCRs) are one of the greatest milestones in organic chemistry. Particularly the procedures described by Suzuki-Miyaura, Sonogashira, Stille or Heck are good examples of this paradigm [1,2], although they all follow different reaction mechanisms. Rapid progress in heterogeneous Pd catalysts for cross-coupling reactions have been realized for the synthesis of compounds for pharmaceutical and chemical industries [3]. The three pillars of heterogeneous catalysis are activity, selectivity and stability. Consequently, it is well established that an ideal heterogeneous catalyst should has high geometric surface area that allow incorporation of high active catalytic sites, mechanical robustness, thermal stability, control loading, negligible leaching, recyclability and any loss of activity by poisoning or deactivation. All these limitations often result in a significant decrease in catalytic activity. Efficient catalyst will clearly require the combination of diverse strategies considering different aspects, such as thermal, mechanical and chemical related with the stability and morphology of the catalyst.

Monolithic catalysts are structures comprising functional interconnected microchannels with a regular three-dimensional structure. They can replace conventional catalysts (homogeneous catalysts) and chemical reactors as well as helping to overcome different problems posed by traditional systems. Monolith reactors were initially developed in mid 1970s for the automotive industry to remove NO, CO and hydrocarbons through gas-solid reactions in engine emission converters. In solution phase chemistry, the monoliths have many advantages over heterogeneous powdery catalytic systems (polymeric reagents, nanoparticles, in general, supported reagents) and traditional packed-bed reactors, such as high transport rates of heat and mass per unit pressure drop, small transverse temperature gradients ease of scale-up and work-up (avoiding filtration processes) [4,5]. When a monolithic catalyst

* Corresponding author.
** Corresponding author.
E-mail addresses: alvaro.gil@usc.es (A. Gil), albertojose.coelho@usc.es (A. Coelho).

https://doi.org/10.1016/j.mtchem.2022.101355

is considered as an alternative to a fixed-bed reactor packed with commercially available catalyst particles, a straightforward prototyping and development program is needed to produce the monolithic catalyst.

Beyond the importance of the catalyst itself in organic reactions, microwave heating has several applications in almost every field of chemistry, due to the advantages that this technology offers compared to traditional heating methods. Microwave assisted organic synthesis (MAOS) has rapidly gained acceptance as a valuable tool for accelerating drug discovery and development processes [6]. Advantages of microwave heating over conventional heating stem mainly from its ability to interact with the material at the molecular level. Heat losses (conductive and convective) associated with traditional heating methods are negligible with microwave heating [7,8]. However, this synthetic methodology is not without risks. In the case of catalysts with metal loadings, microwave-metal discharge could trigger hot-spot formation, local microplasmas and arcing at metal sites, generating hazardous conditions in the presence of flammable solvents and/or gas [9]. These phenomena can cause sparkling or flame inside the microwave reactor. Explosions could occur, for example, in the case of homogeneous PCCCRs using common palladium reagents. These processes are particularly critical at points in the reactor where metal palladium deposits become embedded in the reactor wall in the absence of solvent and therefore under the direct action of microwave radiation [10]. The sparkling phenomena in metal-solvent mixtures has been reviewed by Kappe [11] and co-workers supporting the data reported by Hulshof [12] who observes that arcing phenomena is basically linked to large metal particles. Consequently, an effective immobilization of palladium species on a monolithic catalyst must be taken to avoid metal leaching, hot-spots formation, sparkling and electric discharges in PCCCRs under MAOS.

Cermet is a composite material made up of ceramic materials and metals. Cermets are used to combine the high temperature and abrasion tolerance qualities of ceramics with the malleability of metals. The combination of a heterogeneous cermet-type catalyst with the microwave heating tool has many advantages. Most of the solid catalysts highly absorb microwave irradiation thus they can be considered as an internal heat source. In fact, a way in which microwaves can be selective is by heating a certain part of the catalyst better than the rest. For instance, low-dielectric loss materials such as alumina loaded with microwave active metal (Fe, Pt, Mo or Pd). The microwave active material will heat to very high temperatures leading to selective overheating of metallic sites that cause increased reaction rates [13]. For Mars van Krevelen mechanism [14], where the catalyst surface itself is an active form of the reaction, forming a thin layer of metal-reactant (metal-oxide, metal-sulfide etc.) on the surface, microwave heating causes selective acceleration of primary reaction step, resulting in increased overall rate of reaction [15].

Most cermet manufacturing processes are based on powder metallurgy techniques. Metal and ceramic powders are mixed and ground together in a ball mill or an attrition mill. A lubricant or humectant is often added to facilitate shaping operations. In many cases, after grinding, a suspension is prepared with the raw materials, which is atomized to obtain fine, homogeneous and spherical particles. The pieces are formed by compacting the powder by cold pressing, cold isostatic pressing, or hot isostatic pressing. Except in the latter case, the pieces already formed are thermally processed for sintering at high temperatures in continuous or discontinuous furnaces, with or without controlled atmospheres, depending on the case. Numerous studies have been performed using a support material where the active metal phase is incorporated by impregnation [16–18], absorption [19], deposition-precipitation [20], ion exchange [21] and encapsulation [22,23] process. Some of these methods are usually followed by a thermal or chemical treatment to activate the metal. However, these strategies have their own limitations in terms of design, loading and mechanical/thermal stability.

A highly promising technique for the fabrication of structured catalyst is the 3D printing, an additive manufacturing technique [24,25]. It has been widely used to generate complex-shaped structures with controlled composition and architecture. This approach is based on the extrusion of ink through a nozzle, which can be deposited over a substrate in a layer-by-layer sequence. Owing to the spatial resolution that can be achieved, this technique can be extended to a broad range of technological applications ranging from optoelectronics [26–29], catalysis [30–33], to biomaterials [34–36]. These functional structures can be fabricated using different materials such as metals, ceramics, metal oxides, hydrogels, and composites. The ability to fabricate 3D structures with micrometer resolutions at both meso- and micro-scale depends basically on the rheological behaviour inks and printing parameters. In this respect, the control over these features is fundamental to allow the development of 3D structures with controlled composition, architecture, and specific properties.

In previous works of our research group, we have carried out the manufacture of monoliths using 3D-printing technology, following different strategies such as robocasting and sintering for the manufacture of composite materials based on alumina and copper oxide [30]. In other works, the surface functionalization of SiO_2 monoliths was carried out by silanization and metalation [37], coating with polyimide-palladium composite on the surface [38] as well as incorporation of metallic catalytic species on the surface using the strong electrostatic adsorption technique [39]. To our knowledge, there are no examples of monolithic cermet-type catalysts, manufactured by 3D-printing, tailored to a microwave reactor-vessel. In this work, we present the design and fabrication of the first Pd^0/Al_2O_3 cermet monolithic catalyst [40] specifically designed to fit in a microwave reactor. The catalyst can be rapidly prepared via combination of 3D printing (direct ink writing technique) and subsequent thermal treatment, without any other type of surface treatment after sintering. The catalyst, with 3D structured morphology and long-term stability, was used as an efficient, extremely robust and safe catalyst for Suzuki, Stille, Sonogashira and Heck palladium catalyzed cross-coupling reactions assisted by microwave heating.

2. Experimental section

2.1. Ink synthesis

The ink is synthetized using a protocol similar to that previously described [30]. Briefly, 5 g of $PdCl_2$ (on a stoichiometric basics, 99.9%, Alfa Aesar) was dissolved in 14 mL of deionized (DI) water. Then 50 g of Al_2O_3 powder (mean particle size 0.5 μm and real density of 3.96 g/mL, Almatis GmbH, Germany) was added into the $PdCl_2$ solution, and mixing in a planetary mixer (ARE-250, Thinky, USA) at 2000 rpm for 2 min. After, 0.065 g of (hydroxypropyl) methyl cellulose (HPMC, viscosity 2600–5600 cP, Sigma-Aldrich) was added to the suspension, followed by through mixing at 2000 rpm for 2 min. After 1 h equilibrium, the resulting suspension was gelled by adding 0.13 mL of polyethylenimine (PEI, Mw = 2000, Sigma-Aldrich), and was again homogenized in the planetary mixer at 2000 rpm for 2 min. This mixing process is repeated until to obtain the desired homogeneity. The final printable ink was composed of 5.6 wt% of Pd (relative to the ceramic content) and a ceramic concentration of about 45 vol%.

2.2. Fabrication of Pd^0/Al_2O_3 catalyst

A robotic deposition apparatus (Model A3200, Aerotech Inc., USA) was used to fabricate the catalyst sample. The ink was loaded into the syringe (3 mL, Nordson EFD Inc., Japan), which is attached by a nozzle tip (410 μm diameter size, Nordson EFD Inc.). An air dispenser (Performus VII attached to HP7x, Nordson EFD Inc.) is used to control the ink flow rate. The ink was extruded (Direct Ink Writing) under pressures ranging from of 7–10 bar at a speed of 3–5 mm/s. Catalytic structures were designed using CAD software (Robocad 3.4, 3D Inks, USA), with cylindrical shape (diameter 10 mm and height 5 mm), and open square pores of 590 × 590 μm. After drying at room temperature, the samples were sintered in air at 1500 °C for 2 h with a ramp rate of 10 °C/min.

2.3. Characterization of Pd^0/Al_2O_3 catalyst

The surface morphology and microstructure of the samples were characterized using scanning electron microscopy (SEM, JEOL 6400, JEOL Corporation, Japan) and stereomicroscope (OlympusSZX12, Olympus, Japan). The surface elemental analysis of sintered samples was measured using energy dispersive X-ray spectrometer (EDS, AZTEC/Xact, Oxford, UK). The crystal structure of samples was monitored by a Siemens D5000 diffractometer (Siemens, Germany) with CuKα radiation ($\lambda = 0.15418$ nm). Data was collected in the range of 20–90° (2θ) with a step size of 0.05°. The palladium content in the monolith catalyst was determined by inductively coupled plasma-optical emission spectroscopy (ICP-OES, Varian Liberty 200). Temperature programmed reduction (TPR): The reducible species formed during the calcination step were determined by this technique using an Autosorb 1C-TCD equipped with a thermal conductivity detector. The monolith was loaded in U shaped quartz tube and heated from room temperature to 473 K for 1 h in Ar stream (30 mLN/min). The sample was then cooled down to 313 K and the Ar was replaced by a 5 vol % H_2/Ar gas stream (45 mLN/min). The sample was heated from 313 K to 673 K, at a ramp rate of 10 K/min. CO chemisorption (CO–C): The metal dispersion was measured by CO pulse chemisorption using an AutoChem II 2920 apparatus equipped with a TCD detector. The analysis started by heating the catalysts sample from room temperature to 673 K at 10 K/min under 40 mLN/min of 5 vol % H_2/Ar flow. Then, the sample was kept under 50 mL/min of helium for 30 min and cooled down to 308 K. Finally, when the detection baseline was stable, CO pulse chemisorption started. The dosage was repeated every 2 min until equal peaks were detected or 20 dosages were carried out. Metal dispersion was determined by assuming a stoichiometric ratio of Pd/CO = 1. For surface analysis, X-ray photoelectron spectroscopy (XPS) was carried out using a Physical Electronics PHI 5700 spectrometer with nonmonochromatic Mg Kα radiation (300 W, 15 kV, 1253.6 eV) as the excitation source. High-resolution XPS spectra were recorded at a given take-off angle of 45° by a concentric hemispherical energy electron analyzer, operating in the constant pass energy mode at 29.35 eV, using a 720 μm diameter analysis area. Adventitious carbon at 284.8 eV has been used for charge referencing. Images of Pd nanoparticles dispersed in the ceramic matrix were acquired using a Gemini-500 Field-Emission Scanning Electron Microscope (FESEM) operating at 20 kV using a back-scattering AsB detector with a size resolution of ±0.5 nm. Selected images were analyzed by counting more than 100 particles using ImageJ software.

2.4. Catalytic evaluation

All reactions were performed in a CEM/DISCOVER SP-D-Closed Vessel Microwave apparatus. Iodoarenes, 5-haloisatins, alkenes, alkynes, boronic acids and organotin reagents were purchased from Aldrich and Alfa Aesar [(4-methoxicarbonyl)phenylboronic acid)]. All reactions were monitored by TLC with 2.5 mm Merck silica gel GF 254 strips and the purified compounds showed a single spot. Detection of compounds was performed by UV light and/or iodine vapor. Purification of isolated products was carried out by preparative TLC using silica gel plates. The synthesized compounds were characterized by spectroscopic and analytical data. The NMR spectra were recorded on Bruker AM 300 MHz (^{1}H) and XM500 spectrometers. Chemical shifts are given as δ values against tetramethylsilane as internal standard and *J* values are given in Hz. Proton and carbon nuclear magnetic resonance spectra (^{1}H NMR) were recorded in $CDCl_3$. Melting points were determined on a Gallenkamp melting point apparatus and are uncorrected. Mass spectra were obtained on a Varian MAT-711 instrument. High resolution mass spectra (HR-MS) were obtained on an Autospec Micromass spectrometer.

General procedures for PCCCRs: All reactions were performed using the 3D printed Pd^0/Al_2O_3 cermet monolithic catalyst [total content of Pd on monolithic surface: 1.1 mg; it means 1.1% mmol Pd on the reaction]. No magnetic bar was used in these experiments although they are compatible in these procedures.

2.4.1. Suzuki reactions

In a capped microwave reactor vessel (13 mm internal diameter), provided with the 3D-printed Pd^0/Al_2O_3 cermet catalyst were dissolved the corresponding haloarene (0.98 mmol), Na_2CO_3 (2.94 mmol) and the boronic acid (1.07 mmol) in a mixture of iPrOH/H_2O (2:1 ratio, 5 mL). The mixture was heated at 120 °C under microwave irradiation (200 W) for 20 min. Once the reaction finished, the catalyst was removed from the vial, sonicated, washed with water (5 mL), MeOH (5 mL) and acetone (5 mL) and dried under vacuum for 30 min for reuse. The mixture was washed with water and extracted in AcOEt. The organic phase was dried with anhydrous Na_2SO_4 and evaporated at room temperature on a rotary evaporator. The resulting solid was recrystalized by isopropanol to give the final products compounds **2a-e** (entries 2a-d)].

2.4.2. Sonogashira reactions

In a microwave reactor vessel (13 mm internal diameter), provided with the 3D-printed Pd^0/Al_2O_3 cermet catalyst were dissolved the corresponding iodoarene (0.98 mmol), TEA (2.94 mmol) and the alkyne (1.07 mmol) in iPrOH (5 mL). The mixture was heated at 120 °C in a microwave reactor (200 W) for 30 min. Once the reaction was finalized, the catalyst was removed from the vial, sonicated, washed with water (5 mL), MeOH (5 mL) and acetone (5 mL) and dried under vacuum for 30 min for reuse. The mixture was washed with water and extracted in AcOEt. The organic phase was dried with anhydrous Na_2SO_4 and evaporated at room temperature on a rotary evaporator. The mixture was purified by preparative TLC (AcOEt/Hexane) to give compounds **2f-i**.

2.4.3. Heck reactions

In a microwave reactor vessel (13 mm internal diameter), provided with the 3D-printed Pd^0/Al_2O_3 cermet catalyst were dissolved the corresponding iodoarene (0.98 mmol), TEA (2.94 mmol) and the alkyne (1.07 mmol) in MeCN (5 mL). The mixture was heated at 120 °C in a microwave reactor (300 W) for 20 min. Once the reaction was finalized, the catalyst was removed from the vial, sonicated, washed with water (5 mL), MeOH (5 mL) and acetone (5 mL) and dried under vacuum for 30 min for reuse. The mixture was washed with water and extracted in AcOEt. The organic phase was dried with anhydrous Na_2SO_4 and evaporated at room temperature on a rotary

evaporator. The mixture was purified by preparative TLC (AcOEt/Hexane) to give compounds **2j, d, k, l**.

2.4.4. Stille reactions

In a microwave reactor vessel (13 mm internal diameter), provided with the 3D-printed Pd^0/Al_2O_3 cermet catalyst were dissolved the corresponding iodoarene (0.98 mmol) and the corresponding organostannane (1.07 mmol), in MeCN (5 mL). The mixture was heated at 120 °C in a microwave reactor (200 W) for 20 min. Once the reaction was finalized, the catalyst was removed from the vial, sonicated, washed with water (5 mL), MeOH (5 mL) and acetone (5 mL) and dried under vacuum for 30 min for reuse. The mixture was washed with water and extracted in AcOEt. The organic phase was dried with anhydrous Na_2SO_4 and evaporated at room temperature on a rotary evaporator. The mixture was purified by preparative TLC (AcOEt/Hexane) to give compounds **2a, e, f, m, n**.

3. Results and discussion

Activity, selectivity and stability of a monolithic catalyst could be positively affected during microwave-assisted heterogeneous catalysis. Consequently, in this work we set as specific objectives: the design of a cermet type monolith catalyst provided with an appropriate design (presence of interconnected channels) (1), simple and direct manufacturing (2), catalytic efficiency (3), chemical and mechanical robustness (4), as well as almost unlimited reusability and safety in MAOS (5). We present here a direct manufacturing process based on 3D-printing (direct ink writing, DIW) of catalytic inks based on α-alumina and palladium species and subsequent sintering of the monolith, to obtain a cermet type monolith Pd^0/Al_2O_3.

3.1. Design of the monolithic structure and the composition of the Pd^0/Al_2O_3 cermet

Monolithic catalyst design: The shape and size of the monolith, to adapt it to a certain reactor, can be modulated by 3D printing, so this technology is ideal in prototyping processes. As can be seen in Figs. 1b,d and 3b,c, the shape of the catalyst is adjusted to the shape and dimensions of the microwave vessel. For this reason, a slightly flattened cylindrical shape structure was designed, adapted to the bottom of the vessel.

Regarding the composition of the final product, it is important to highlight that the material described here contains metallic species both inside the filaments of the structure and on the surface as Pd^0 and not as PdO (oxide). Therefore, the material obtained in this work is a true cermet: metal (0)-ceramic composite, so this monolith is particularly efficient in palladium-catalyzed cross-coupling reactions (Suzuki, Stille, Sonogashira, Heck).

Alumina-based ceramics (Al_2O_3) have excellent physical and chemical properties. In addition, they have good mechanical resistance and thermal stability [41]. However, their high Young's modulus values make the applications somewhat limited due to their high brittleness, as they are not easily deformed. Consequently, alumina ceramics are very sensitive to minimal defects in their microstructure, which acts as a crack initiation point [42,43]. Nevertheless, ceramic materials can improve their fracture toughness by homogeneous incorporation of fine particles of ductile metals in the matrix. Different reinforcement metal amounts of Al_2O_3/Al [44], Al_2O_3/Cr [45], Al_2O_3/Cu [46], Al_2O_3/Ni [47], Al_2O_3/Mo [48], Al_2O_3/Ti aluminide [49] and Al_2O_3/Ni_3Al [50] have been reported. Many of these composites are synthesized using powder techniques. These techniques start from a mixture of powders from a high-energy mechanical grinding, and later they are subjected to a pressing process, and finally they are sintered at a certain time and temperature, giving rise to the composite material [51]. Therefore, the robustness of the monolithic material improves with the incorporation of the metallic component in the composition of the internal matrix of the filaments. It is well known that cermet experiences a decrease in their hardness and elasticity module in comparison with the material base. However, his fracture toughness increases. Consequently, these factors contribute to the new composite better tolerating the generation of cracks when the material is working under conditions of high loads and friction [51].

3.2. Preparation and Characterization of Pd^0/Al_2O_3 catalyst

The synthesis of the monolithic catalyst is very direct and simple since it is a process of 3D-printing and sintering, which is carried out without any other type of surface treatment. Specifically, we first developed an aqueous colloidal Pd/Al_2O_3 ink with tailored rheological properties for 3D printing that contains moderate Pd loading (5.6 wt%). Al_2O_3 has been used as matrix due to its excellent thermal and mechanical properties [52], which leads to obtain a catalyst with remarkably stability. After an appropriate ink synthesis, a 3D structure with high geometric surface area and open square pores was fabricated, followed by thermal annealing at 1500 °C for 2 h to obtain a catalyst with thermal/mechanical integrity. A detailed physico-chemical characterization for the catalyst was carried out by optical, scanning electron microscopy (SEM), EDS, and X-ray diffraction (XRD) techniques, and it was evaluated as catalyst in Suzuki, copper-free Sonogashira, Stille and Heck cross-coupling reactions under microwave heating conditions. The proposed strategy can be extended to other metals, opening new opportunities in the design and synthesis of efficient metal catalyst. Fig. 1 shows the physical parameters and different images of the 3D Pd^0/Al_2O_3 catalyst. This structure was prepared using colloidal Pd/Al_2O_3 ink, where the stabilization of Pd in the sample combines chemical and physical strategies. In the first step, concentrated colloidal ink was prepared by using a Pd^{+2} precursor ($PdCl_2$) that was absorbed into the Al_2O_3 particles through electrostatic interactions in an aqueous solution under stirring. Content of Pd could be adjusted in this step by varying the amount of the metal precursor. Particularly, we created ink with a weight percentage of 5.6 wt% Pd to achieve sufficient reinforcement in the internal structure, as well as a minimum palladium content on the surface, necessary for catalysis to occur. Then, a non-ionic (hydroxypropyl)methyl cellulose (HPMC) and a cationic polyethylenimine (PEI) were added to impart the desired rheological properties to the ink. Subsequently, the obtained ink was used to fabricate the Pd/Al_2O_3 catalyst by 3D printing technique. This catalyst was designed with well-controlled morphology using CAD software, where the size and shape is proportional to the microwave reaction vessel. Finally, as discussed above, the resulting sample was sintered at 1500 °C for 2 h to form a catalyst with remarkable mechanical and structural properties, which are strongly related with the catalytic activity. Note that the thermal treatment was selected, in order to achieve a catalyst with excellent mechanical properties and a specific oxidation state (0) of Pd. At a lower temperature, the catalyst could be easily cracked when the reactions will be carried out under shaking and microwave heating conditions. During the sintering process, no reducing atmosphere was used to get Pd^0 in the cermet. As shown in Fig. 1b–i, the sintered sample present a uniform shape, network structure, and a homogeneous surface without cracks. Fig. 1c shows the sintered structure with interconnected square pores. The cross-sectional image in Fig. 1e confirms the multilayer and interconnected morphology of the final catalyst. The advantages of choosing this

(a)

Physical properties	
Catalytic system	Pd/Al_2O_3
Nature of ceramic	α-Al_2O_3
Active phase	Pd
Geometry support	Woodpile simple cubic
Channel geometry	Square
Height support	0.5 cm
Diameter support	0.8 cm
Geometric surface area (GSA)	33.2 cm^2/cm^3
Wall thickness	291 μm
Pore size	424 μm

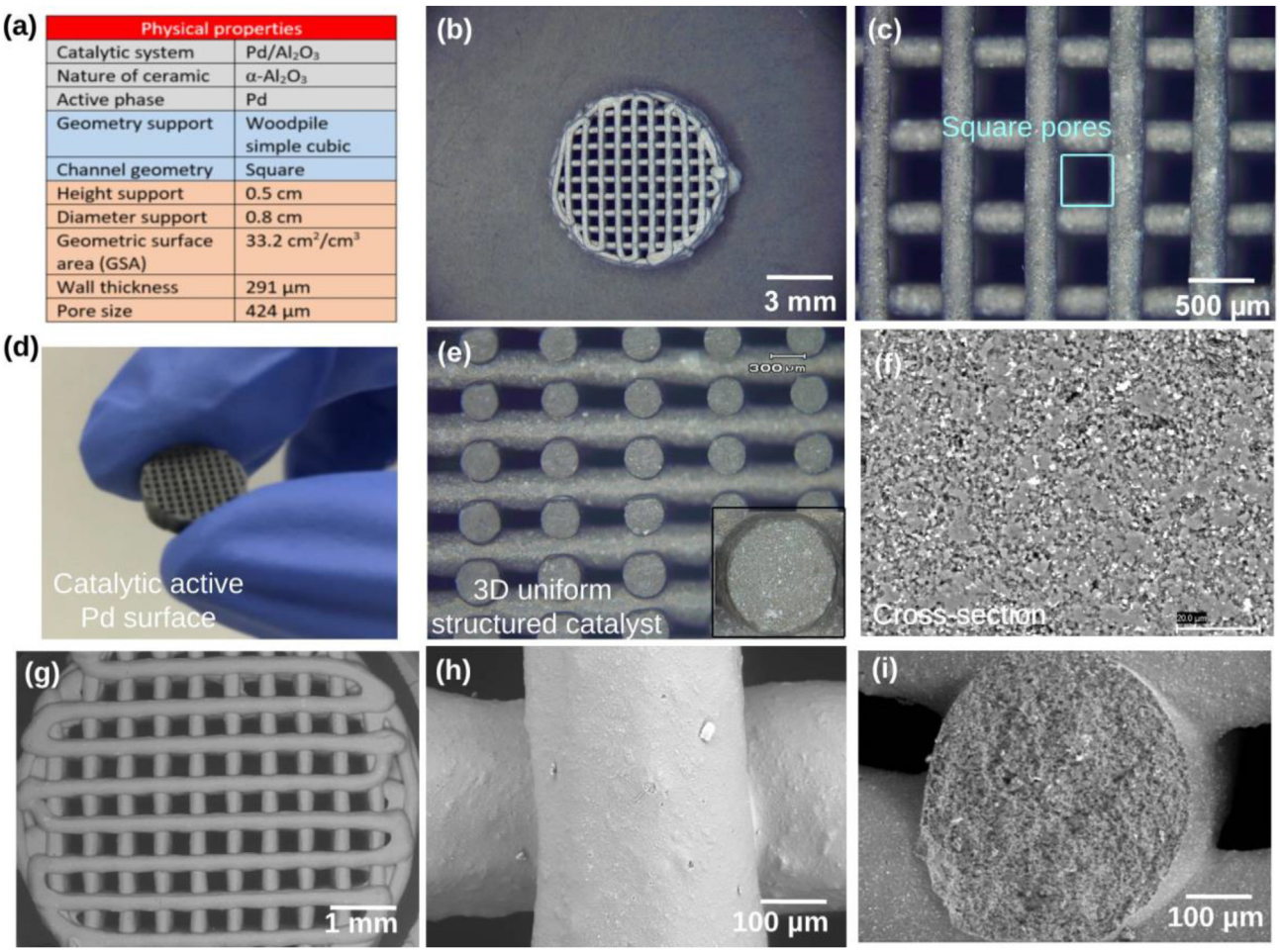

Fig. 1. (a) Physical parameters of the sintered sample. (b) Optical microscopy images of the sample surface after sintering and (c) interconnected square pores. (d) Photograph showing the Pd^0/Al_2O_3 catalyst fabricated with cylinder geometric shape. (e) Optical microscopy cross-sectional image. The inset is a rod with a width of 291 μm. (f) High-magnification SEM image, showing the microporosity on the cross section (internal section). (g, h) SEM images of the smooth external surface of the monolith. (i) SEM image of the filament cross section, showing different appearance between smooth (outer) and rough surface (inner section).

morphology are the formation of high surface area to volume ratio, which enhances the number of active sites for catalytic reactions. Noticeably, the sintered structure is mechanically robust to tolerate long-term and repeated reaction cycles. As expected, the colour of catalyst changed after sintering from light-grey (dried sample) to more black (sintered sample), suggesting an efficient reduction of Pd^{+2} into Pd^0, probably as a consequence of the presence of poly-ethylenimine (PEI), in the catalytic ink, acting as a palladium reducing agent. In addition, moderate diffusion out of the Pd metal through the substrate was observed after sintering, suggesting a significant metal immobilization in the sample. Particularly, the results of the chemical analysis obtained by ICP-OES indicate that metallic content (Pd wt%) is around 1.66 wt% for the sample after sintering. Furthermore, the optimum sintering temperature results in a catalyst with a geometric surface area (surface area-to-volume ratio) of 33.2 cm^2/cm^3, according to the dimensions the external dimensions of structure.

A smooth surface was further confirmed by the magnified SEM image (Fig. 1g and h). The cross section of the monolith (view of the inner cross section of the metal-ceramic composite) is shown in Figs. 1f, i and 2a, where the two materials (metal and ceramic) are observed. In addition, from this image it cannot be observed any segregation or precipitation of the Pd at the grain boundary region, demonstrating that Pd metal was well integrated within the Al_2O_3 matrix.

The qualitative and quantitative distribution of palladium on the monolith surface were experimentally confirmed by the SEM, EDS and mapping, XRD, TPR and CO—C. Fig. 2a shows the surface SEM image of the Pd^0/Al_2O_3 filament, and Fig. 2b represents its spectrum in two different regions. The results, together with the EDS-mapping results (Fig. 2c), reveal that the Pd element is evenly distributed throughout the monolith structure. This outer Pd content is available for the catalytic reactions. The presence of Pd is confirmed in the two regions (inner and outer sections) by the EDS.

These results demonstrated that Pd could be efficiently loaded on the ceramic network with an excellent confinement into the Al_2O_3 matrix after the sintering process. In addition, FESEM images at higher resolution allow to observe that Pd is dispersed along the ceramic matrix surface but also inside their pores in the form of nanoparticles. These appear in the form of aggregates/clusters with a mean size of ca. 185 ± 50 nm (Fig. 2f—h). This agglomeration can result from the sintering of adjacent Pd ions distributed along the matrix during the thermal reduction process due to the absence of any stabilizer to allow control of nucleation and growth. In addition, the clusters seem to be formed by particles/crystallites of lower size. Inspection of selected areas in the acquired images

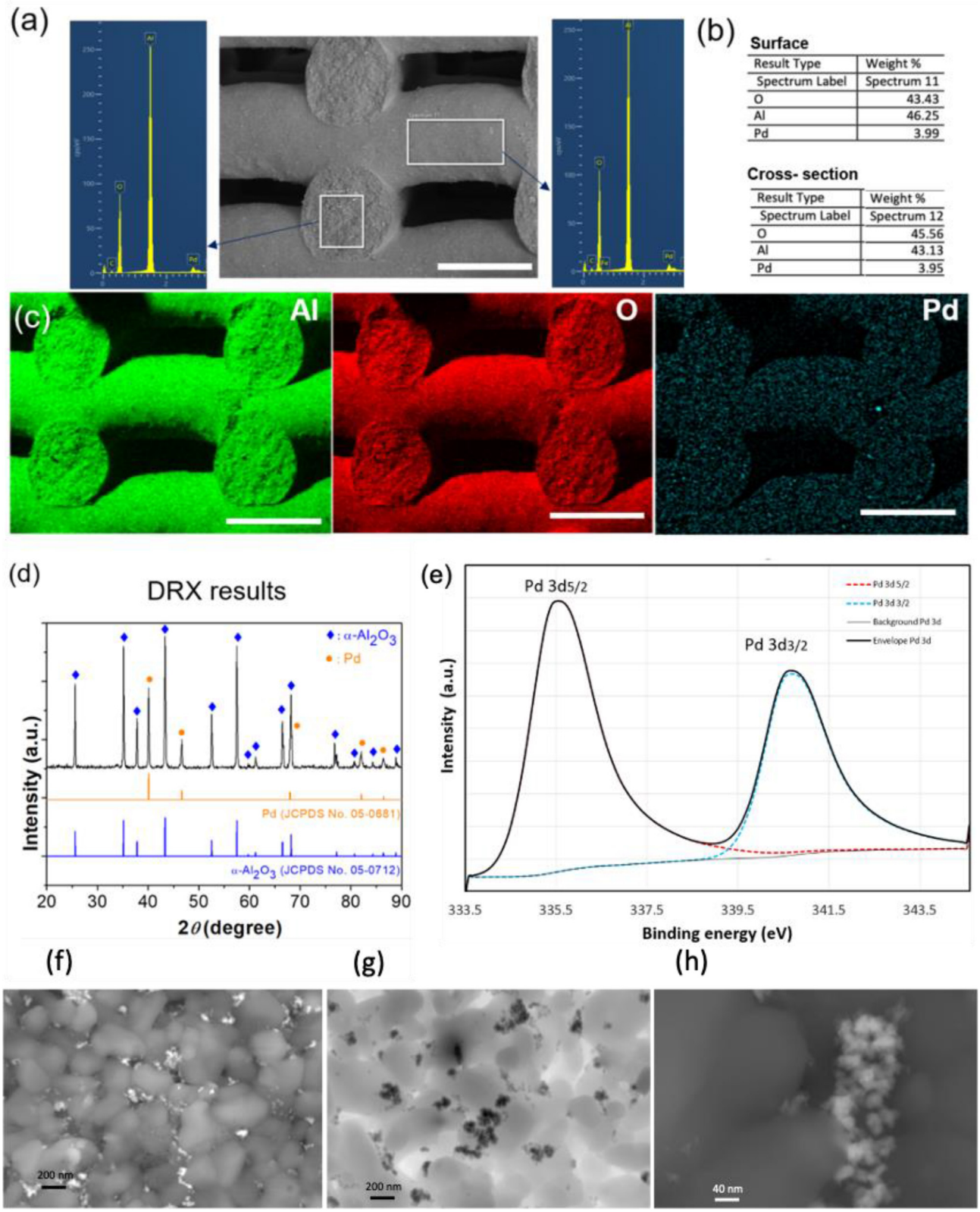

Fig. 2. (a) SEM and EDS spectrum of the Pd^0/Al_2O_3 catalyst surface and internal phase (cross section in detail). (b) Semiquantitative EDS-calculations of the monolith (outer and inner composition). (c) SEM image and EDS elemental mapping of the catalyst, showing the homogeneous distribution of O, Al and Pd. Scale bar 500 μm. (d) XRD pattern of the calcined Pd^0/Al_2O_3 powders. (e) XPS spectra of the monolithic surface catalyst. (f–h) High-resolution FESEM images of Pd nanoparticles dispersed in the ceramic Al_2O_3 matrix collected with an AsB detector (backscattering electrons) at 20 kV.

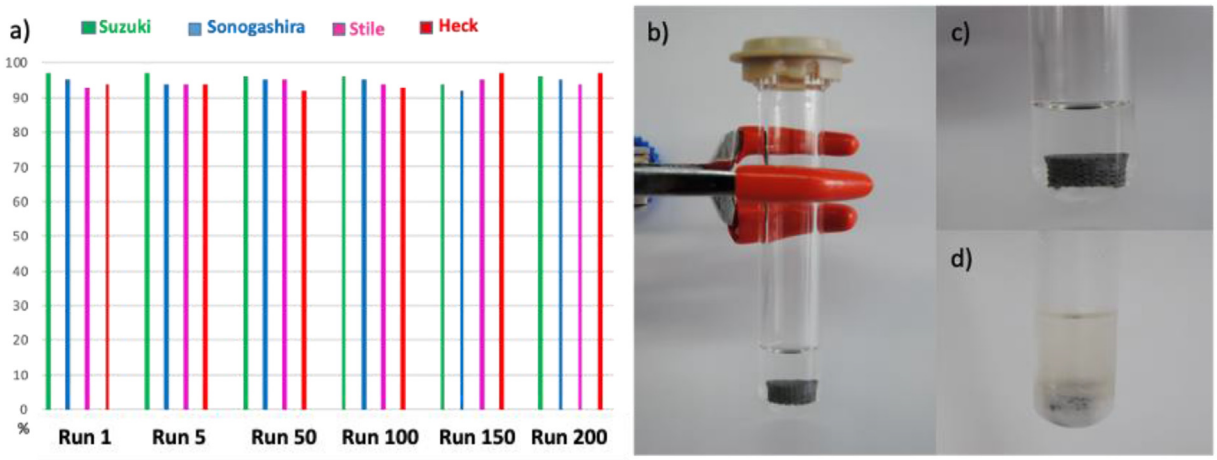

Fig. 3. (a) Recyclability of the four procedures in the first 200 reaction cycles (catalyst used interchangeably in the four different processes). (b, c) Reactor vessel and reaction mixture (Example: Suzuki, synthesis of compound **2d**) before microwave heating. (d) Reaction mix completed, after microwave treatment. The final products crystallize in the reactor vial, after cooling.

provides approximate values of the crystallites composing the particle agglomerates of ca. 40 ± 5 nm.

X-ray diffraction analysis was performed to verify the presence of the Pd on the sample (Fig. 2d). The XRD pattern of the sample shows characteristic peaks of two different phases corresponding to α-Al_2O_3 (JCPDS No. 05−0712) and Pd (JCPDS No. 05−0681). In particular, the peaks observed at 2θ values of 40.11°, 46.64°, 68.19°, 82.05° and 86.4° correspond to (111), (200), (220), (311) and (222) planes of the Pd metal, respectively. These peaks are sharp and well defined, which indicates that the metallic Pd has a high degree of crystallinity. Clearly, there are not obvious diffraction peaks that could be associated to crystalline palladium oxide species or Pd−Al alloys, indicating that the introduction of Pd into the Al_2O_3 not generate Pd complexes during the chosen thermal treatment. Finally, the reduction properties of the monolith were measured by TPR. The obtained TPR profile was flat suggesting that most of the palladium species incorporated was already reduced. Results of the CO chemisorption showed a metal (Pd) dispersion of 0.192% on the surface, which is sufficient and beneficial to carry out MAOS safely. To evaluate the oxidation state of the palladium in the Pd/Al_2O_3 catalyst, XPS was utilized. The high-resolution XPS spectrum (Fig. 2e) reveals the existence of Pd^0, where it showed double peaks with bending energies at 335.5 and 340.8 eV, which correspond to Pd^0, Pd 3d5/2 and Pd 3d3/2, respectively. These results combined with the XRD spectra (Fig. 2d) confirm the presence of Pd^0 on the outer surface of the catalyst.

3.3. Catalytic evaluation of Pd^0/Al_2O_3 cermet catalyst in PCCCRs

3.3.1. Catalytic evaluation in Suzuki, Sonogashira, Stille and Heck reactions

These four reactions follow different mechanisms for the formation of carbon-carbon bonds and have been extensively used in organic chemistry. However, the reaction conditions of homogeneous catalysis are not always extrapolated to heterogeneous catalysis. This fact makes it necessary to carry out an exhaustive screening of the reaction conditions for a new catalytic material. The first studies of the catalytic activity of the monolithic catalyst adapted to the microwave vial (Fig. 3b and c) focused on the following issues: performing PCCCRs in secure MAOS, obtaining selectivity and high yields for the four transformations studied (Suzuki, Sonogashira, Stille and Heck); check for possible palladium leaching on the monolith surface under different reaction conditions (alkenes, alkynes, boronic acids, stannanes, bases and solvents) at high temperature and the reusability of the monolithic catalyst in MAOS. The results of catalytic activity for the four protocols are shown in Table 1. In all reactions, taking into account the total amount of palladium detected on the monolith surface [(0.192% Pd on surface, it means 1,1 mg on the surface (standard monolith weight: 600 mg)], the reactions worked well using 0.98 mmol of starting substrates [4-iodobenzene (**1a**), 4-iodotoluene (**1b**), 4-iodoanisole (**1c**) as well as 5-haloisatins such as 1-benzyl-5-iodoindoline-2,3-dione (**1d**) and 1-benzyl-5-bromoindoline-2,3-dione (**1e**)] and the corresponding coupling partner (boronic acid, alkyne, alkene or stannane) in four different protocols. For the Suzuki reaction, standard conditions were explored using inorganic bases such as sodium carbonate in hydroalcoholic mixtures. The best results were achieved using 3 equiv of base (Na_2CO_3) and iPrOH/H_2O (2:1 ratio) as a solvent mixture, under microwave heating, 200 W at 120 °C, for 20 min, rendering almost quantitative yields. No collateral products were detected during the reactions. Therefore, the selectivity towards the desired products **2a-e** was excellent. As can be observed in Fig. 3d, reaction products frequently crystallize in the microwave vial when the mixture has cooled. The monolith is easily removable from the microwave reactor for reuse after washing and sonication. It is important to point out that during the optimization process of the Suzuki reaction conditions, the presence of two phases is a critical issue for the efficiency of the catalyst. The correct dissolution of all the reagents in a suitable hydroalcoholic phase is required. In this sense, the iPrOH/H_2O mixture proved to be effective for these transformations. iPrOH is stable under normal conditions of use and is completely soluble in water.

The TOF values (Table 1) were calculated using the formula:

$$TOF = \text{mol product} / [\text{time (min)} \times \text{mol catalyst}]$$

TOF values range from 100 to 450h-1, suitable for a sintered catalyst and comparable to other types of palladium-based powdery catalysts. The reactivity of the CERMET catalyst under conventional heating conditions is quite similar, although the final yield of the reactions decreases somewhat, especially the bromo-derivatives. Reaction times are longer too. Other "pseudo heterogeneous" powdery catalysts such as palladium on charcoal give a similar result under conventional heating conditions but are effective for a limited number of cycles. Therefore, under

Table 1
Suzuki, Sonogashira, Heck and Stille reactions using 3D-Pd^0/Al_2O_3 cermet.

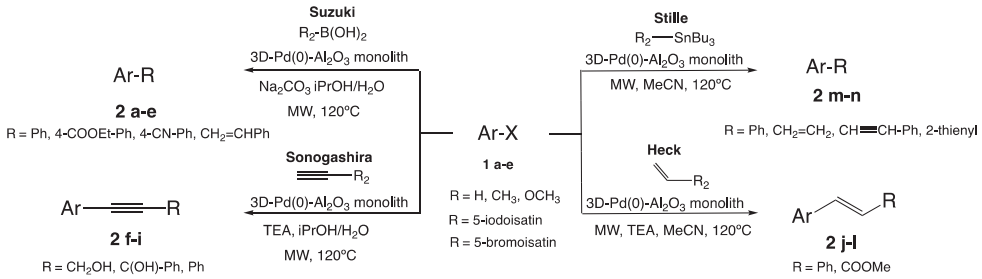

Compound	Aryl halide (1a–e)	Boronic acid/Alkyne Stannane/Alkene	Time (min)	Yield[a] (%), TOF(h)[j]
2a		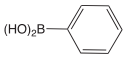	20	96[b,c], 95[h], 272[j]
2b		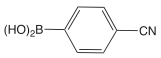	20	97[b,c], 274[j]
2c		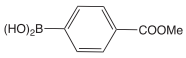	20	92[b,c], 260[j]
2d	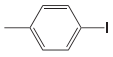	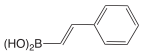	20	97[b,c], 95[i], 171[j]
2e	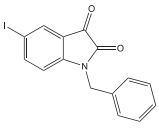	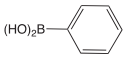	30	98[b,c], 96[h], 102[j]
2e	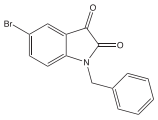	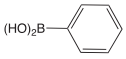	30	90[b,c], 90[h], 104[j]
2f		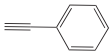	30	94[b,d], 92[h], 177[j]
2g	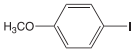		30	88[b,d], 145[j]
2h			20	90[b,d], 255[j]
2i	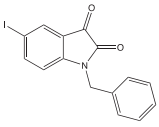	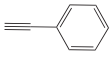	30	93[b,d], 92[h], 98[j]
2i	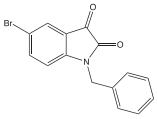	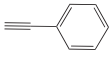	30	91[b,d], 90[h], 110[j]
2j		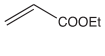	20	93[e,f], 93[h], 260[j]
2d	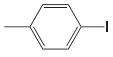		20	93[e,f], 246[j]
2k		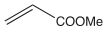	10	92[e,f], 95[i], 267[j]
2l	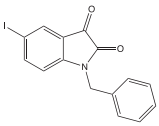	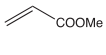	10	95[e,f], 302[j]

Table 1 (*continued*)

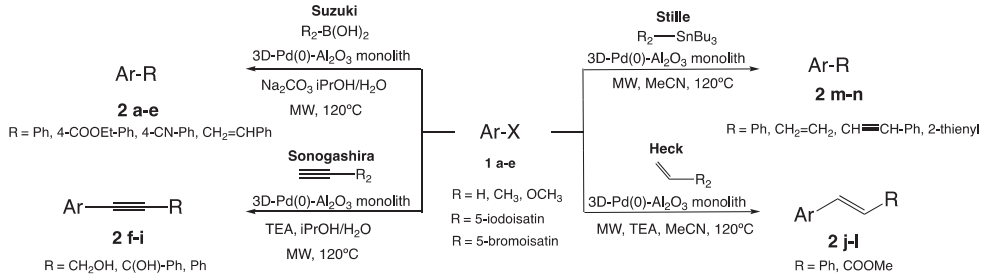

Compound	Aryl halide (1a–e)	Boronic acid/Alkyne Stannane/Alkene	Time (min)	Yield[a] (%), TOF(h)[j]
2m			10	80[b,g], 450[j]
2f		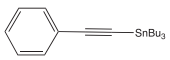	30	90[b,g], 95[i], 179[j]
2a		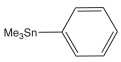	30	92[b,g], 90[h], 181[j]
2e	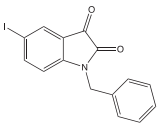	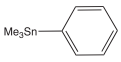	20	98[b,g], 97[h], 154[j]
2e	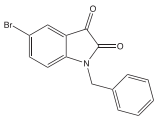	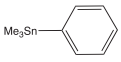	20	95[b,g], 95[h], 173[j]
2n	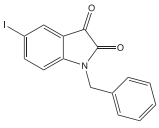	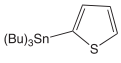	20	95[b,g], 95[h], 148[j]
2n	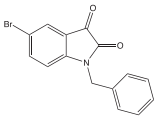	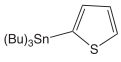	20	93[b,g], 92[h], 170[j]

[a] Isolated yield. All reactions were carried out in a microwave reactor vessel and a 3D-Pd^0/Al_2O_3 monolithic cermet (1% mol Pd).
[b] 200W, 120 °C.
[c] Suzuki conditions: iodoarene or haloisatin (0.98 mmol), Na_2CO_3 (2.94 mmol), boronic acid (1.07 mmol), iPrOH/H_2O.
[d] Sonogashira conditions: iodoarene or haloisatin (0.98 mmol), TEA (2.94 mmol), alkyne (1.07 mmol), iPrOH/H_2O.
[e] Heck conditions: iodoarene or haloisatin (0.98 mmol), alkene (1.07 mmol), TEA (2.94 mmol), MeCN.
[f] 300W, 120 °C.
[g] Stille conditions: iodoarene or haloisatin (0.98 mmol), stannane (1.07 mmol), MeCN.
[h] Yield after 30 cycles.
[i] Yield after 200 cycles.
[j] TOF = mol product/[t (h) × mol catalyst].

microwave heating conditions, the cermet behaved with good performance and, what is not less important: safe reaction conditions, without risk of explosion due to the presence of palladium inside the reactor. Therefore, this catalyst could be used in even more challenging reactions in which MAOS is especially required.

In Sonogashira reactions, the best conditions for the copper-free coupling between iodoarene or haloisatin derivatives with simple terminal alkynes were studied. The best results were obtained using triethylamine (TEA) as base and iPrOH/H_2O as solvents (200 W, 120 °C). As shown in Table 1, the reactions were performed in 20 min and with high yields. Finally, Heck and Stille reactions were carried out using acetonitrile (MeCN) as a suitable solvent for these transformations, with short reaction times, at 120 °C. Organostannanes react efficiently using standard conditions (20W, 120 °C), in 10–30 min. In the case of Heck reactions, an increase in power (300W) was necessary to complete the reactions. The catalyst can carry out every reaction described here without the need to incorporate the magnetic stirrer into the microwave reactor. In this way, the reactants flow through the catalyst channels through the simple action of microwave energy (Fig. 3b). The work-up is very simple since no filtration process is necessary. The monolithic catalysts prepared and used in this work were reused, indistinctly in the four procedures, for hundreds of times without appreciable loss of catalytic activity. In addition, the catalyst was completely safe under microwave heating conditions. No sparkling or arcing phenomena were detected during these experiments. Fig. 3a shows the recyclability diagram for the first six cycles for each transformation, taking as

model reactions those aimed at obtaining compounds **2a** (Suzuki or Stille), **2e** (Sonogashira), or **2h** (Heck). This fact, together with the strong mechanical resistance offered by the catalyst (without fractures, scratches, breaks or surface poisoning) define this cermet system as a true "long-life catalytic material".

3.3.2. Evaluation of leaching. Hot filtration test and ICP results

To determine if the monolithic catalyst works through a true heterogeneous catalysis, several studies were carried out. On the one hand, the Inductive Coupling Plasma (ICP/OES) results, measured in the reaction crudes (Suzuki, Sonogashira, Heck or Stille), showed that the Pd concentration in the reaction solution was less than the detection limit (i.e., 50 ppb) which corresponds to less than 0.02% of the starting Pd-amount (see S4 supplementary material). Secondly, the overwhelming reusability discussed above (each monolithic catalyst can work for hundreds of times in different reaction solvents) shown by the catalyst demonstrates the excellent possible applicability of this device in parallel drug synthesis (in which the presence of traces of metal is absolutely avoided). Third, the graph corresponding to the CO chemisorption made after carrying out numerous catalysis experiments was identical to the initial one (see S3 supplementary information), so it can be considered that the dispersion of the metal on the surface remains constant after numerous reaction cycles. Finally, hot filtration tests (HFT) (see S4, supplementary material) were performed for the four methods. Every experiment showed the absence of catalysis when the monolith is removed from the reaction mixture. The results of these tests indicated that the metal leaching is negligible or undetectable under the applied reaction conditions.

3.3.3. Mechanical properties of the catalysts: robustness and mechanical strength

In addition to the factors related to chemical resistance discussed above, it is worth highlighting the great mechanical robustness, demonstrated by the total absence of fractures on the surface after 200 reaction cycles (see tables S3, supplementary material). It is important to point out that, although the exact determination of the mechanical properties of the monolith is not an objective for this work, we have compared the robustness of the Pd^0/Al_2O_3 cermet catalyst with other previously reported catalysts[38-40] that contain palladium on the monolith surface but do not present palladium content throughout its internal structure. This comparison has been made based on the presence of fractures on the catalyst surface and the maximum number of times each monolith can be reused in solution phase cross coupling reactions. These studies indicate that cermet is much more resistant, robust and durable than catalysts that do not have internal metal content, due to a much lower degree of internal crystallinity than monoliths internally composed of pure Al_2O_3 or SiO_2. (see table S3 in supplementary material).

4. Conclusions

In summary, we have developed a strategy for the fabrication of an efficient and robust Pd^0/Al_2O_3 cermet catalyst for use in safe Suzuki, Sonogashira, Stille and Heck protocols in microwave assisted cross-coupling reactions. Combining 3D printing technology and thermal annealing, it is possible to obtain a monolithic catalyst with open square pores, high geometric surface area of 33.2 cm^2/cm^3, uniform Pd loading after sintering of 1.66 wt% and increased robustness related to pure ceramic monoliths. EDS and mapping analysis confirmed the homogeneous distribution of Pd metal on the structure surface. Due to the synergistic effects of the metal-oxide interfaces, the monolithic catalyst is highly efficient and extremely robust in organic mixtures with aqueous solvents and high temperatures and Pd leaching was completely undetected by HFT or ICP/OES. The versatility of our fabrication approach provides an efficient strategy for the development of safe microwave-assisted cross-coupling reactions in the presence of a metal catalyst. In addition, the immobilized Pd catalyst could be easily washed, reused and applied safely as a "long-life catalytic device" in 200 different cross coupling reaction experiments without arcing phenomena, catalyst deactivation, surface poisoning or structural damage.

CRediT author statement

The corresponding author is responsible for ensuring that the descriptions are accurate and agreed by all authors.

Carmen R. Tubio: Investigation, Writing- Original draft preparation. Camilla Malatini: Investigation. Laura Barrio: Investigation. Christian F. Masaguer: Supervision. Manuel Amorín: Data Curation Management. Walid Nabgan: Data Curation Management. Pablo Taboada: Resources, Data Curation Management. Francisco Guitián: Funding acquisition, Resources. Alvaro Gil: Conceptualization Ideas, Supervision. Alberto Coelho: Conceptualization, Management and coordination responsibility for the research activity planning and execution, Writing- Original draft preparation, Writing- Reviewing and Editing, Funding acquisition.

Declaration of competing interest

The authors declare that they have no known competing financial interests or personal relationships that could have appeared to influence the work reported in this paper.

Data availability

Data will be made available on request.

Acknowledgements

This work was financially supported by the Consellería de Cultura, Educación e Ordenación Universitaria of the Galician Government: EM2014/022 to A.C., ED431B2016/028 to F.G. The Strategic Grouping AEMAT grant No. ED431E2018/08 and the Spanish Ministry of Science, Innovation and Universities with grant No: MAT2017-90100-C2-1-P "MA thanks Xunta de Galicia and the ERDF (ED431C 2021/21)".

Appendix A. Supplementary data

Supplementary data to this article can be found online at https://doi.org/10.1016/j.mtchem.2022.101355.

References

[1] S. Sain, S. Jain, M. Srivastava, R. Vishwakarma, J. Dwivedi, Curr. Org. Synth. 16 (2019) 1105–1142.
[2] C. Barnard, Platin. Met. Rev. 52 (2008) 38–45.
[3] M. Pagliaro, V. Pandarus, R. Ciriminna, F. Béland, P. DemmaCarà, ChemCatChem 4 (2012) 432–445.
[4] H. Yue, Y. Zhao, L. Zhao, J. Lv, S. Wang, J. Gong, X. Ma, AIChE J. 58 (2012) 2798–2809.
[5] J.A. Moulijn, M.T. Kreutzer, T.A. Nijhuis, F. Kapteijn, Adv. Catal. 54 (2011) 249–327.
[6] A. Tapas, D.D. Magar, P. Kawtikwar, D.M. Sakarkar, R.B. Kakde, Int.J. PharmTech Res. 1 (2009) 1039–1050.
[7] S. Horikoshi, N. Serpone, Catal. Sci. Technol. 4 (2014) 1197–1210.
[8] J.P. Tierney, P. Lidström (Eds.), Microwave Assisted Organic Synthesis, Blackwell Publ./CRC Press, Oxford, 2005.
[9] A. Gavin Whittaker, D. Imichacl, P. Mingos, J. Chem. Soc., Dalton Trans. (2000) 1521–1526.
[10] C.O. Kappe, A. Stadler, Microwaves in Organic and Medicinal Chemistry, first ed., Wiley VCH, Weinheim, 2005.

[11] W. Chen, B. Gutmann, C.O. Kappe, ChemistryOpen 1 (2012) 39–48.
[12] M.H.C.L. Dressen, B.H.P. Van De Kruijs, J. Meuldijk, J.A.J.M. Vekemans, L.A. Hulshof, Org. Process Res. Dev. 11 (2007) 865–869.
[13] X. Zhang, D.O. Hayward, D.M.P. Mingos, Catal. Letters 88 (2003) 33–38.
[14] J.R.H. Ross, Contemp. Catal. (2019) 161–186.
[15] P.D. Muley, Y. Wang, J. Hu, D. Shekhawat, Microwave-Assisted Heterogeneous Catalysis, 2021.
[16] J. Lichtenberger, D. Lee, E. Iglesia, Phys. Chem. Chem. Phys. 9 (2007) 4902–4906.
[17] Y. Tonbul, S. Akbayrak, S. Özkar, Int. J. Hydrogen Energy 41 (2016) 11154–11162.
[18] H. Bahruji, M. Bowker, G. Hutchings, N. Dimitratos, P. Wells, E. Gibson, W. Jones, C. Brookes, D. Morgan, G. Lalev, J. Catal. 343 (2016) 133–146.
[19] M.E. Martínez-Klimov, P. Hernandez-Hipólito, T.E. Klimova, D.A. Solís-Casados, M. Martínez-García, J. Catal. 342 (2016) 138–150.
[20] W.J. Shen, Y. Matsumura, J. Mol. Catal. Chem. 153 (2000) 165–168.
[21] L. Duan, R. Fu, B. Zhang, W. Shi, S. Chen, Y. Wan, ACS Catal. 6 (2016) 1062–1074.
[22] H. Kaur, D. Shah, U. Pal, Catal. Commun. 12 (2011) 1384–1388.
[23] W.R. Reynolds, P. Plucinski, C.G. Frost, Catal. Sci. Technol. 4 (2014) 948–954.
[24] J.A. Lewis, Adv. Funct. Mater. 16 (2006) 2193–2204.
[25] Y. Zhang, F. Zhang, Z. Yan, Q. Ma, X. Li, Y. Huang, J.A. Rogers, Nat. Rev. Mater. 2 (2017) 17019.
[26] C.R. Tubío, J.A. Nóvoa, J. Martín, F. Guitián, J.R. Salgueiro, A. Gil, RSC Adv. 6 (2016) 2450–2454.
[27] J.J. Adams, E.B. Duoss, T.F. Malkowski, M.J. Motala, B.Y. Ahn, R.G. Nuzzo, J.T. Bernhard, J.A. Lewis, Adv. Mater. 23 (2011) 1335–1340.
[28] J. Pyo, J.T. Kim, J. Lee, J. Yoo, J.H. Je, Adv. Opt. Mater. 4 (2016) 1190–1195.
[29] B.Y. Ahn, E.B. Duoss, M.J. Motala, X. Guo, S. Park, Y. Xiong, J. Yoon, R.G. Nuzzo, J.A. Rogers, J.A. Lewis, Science 323 (2009) 1590–1593.
[30] C.R. Tubío, J. Azuaje, L. Escalante, A. Coelho, F. Guitián, E. Sotelo, A. Gil, J. Catal. 334 (2016) 110–115.
[31] J. Azuaje, C.R. Tubío, L. Escalante, M. Gómez, F. Guitián, A. Coelho, O. Caamaño, A. Gil, E. Sotelo, Appl. Catal. Gen. 530 (2017) 203–210.
[32] J.N. Stuecker, J.E. Miller, R.E. Ferrizz, J.E. Mudd, J. Cesarano, Ind. Eng. Chem. Res. 43 (2004) 51–55.
[33] X. Zhou, C.-J. Liu, Adv. Funct. Mater. 27 (2017) 1701134.
[34] S.-I. Roohani-Esfahani, P. Newman, H. Zreiqat, Sci. Rep. 6 (2016) 19468.
[35] B. Leukers, H. Gülkan, S.H. Irsen, S. Milz, C. Tille, M. Schieker, H. Seitz, J. Mater. Sci. Mater. Med. 16 (2005) 1121–1124.
[36] L. Sweet, Y. Kang, C. Czisch, L. Witek, Y. Shi, J. Smay, G.W. Plant, Y. Yang, PLoS One 10 (2015) 1–19.
[37] A.S. Díaz-Marta, C.R. Tubío, C. Carbajales, C. Fernández, L. Escalante, E. Sotelo, F. Guitián, V.L. Barrio, A. Gil, A. Coelho, ACS Catal. 8 (2018) 392–404.
[38] A. Sanchez Díaz-Marta, S. Yáñez, C.R. Tubío, V.L. Barrio, Y. Piñeiro, R. Pedrido, J. Rivas, M. Amorín, F. Guitián, A. Coelho, ACS Appl. Mater. Interfaces 11 (2019) 25283–25294.
[39] A.S. Díaz-Marta, S. Yañez, E. Lasorsa, P. Pacheco, C.R. Tubío, J. Rivas, Y. Piñeiro, M.A.G. Gómez, M. Amorín, F. Guitián, A. Coelho, ChemCatChem 12 (2020) 1762–1771.
[40] F. Guitian Rivera, A. Gil Gonzalez, C. Rial Tubio, E. Sotelo Pérez, J.A. Coelho Cotón, Patent WO 2021/089901, 2021.
[41] J.G. Miranda, Efecto Del Contenido de Cu En Las Propiedades Mecánicas y Resistencia Eléctrica de Un Material Compuesto Base Al_2O_3, UAM-A, México, 2006.
[42] C.P. Rebolledo, R. Jimenez, Ciencia de Materiales: Teoría, Ensayos, Tratamientos, eleventh ed., Pirámide, Spain, 2000.
[43] J.M. Meza, Tenacidad a La Fractura En Cerámicos, Universidad Nacional de Colombia Sede Medellín, 2001.
[44] K. Konopka, M. Szafran, J. Mater. Process. Tech. 1–3 (2006) 266–270.
[45] M. Chmielewski, K. Pietrzak, J. Eur. Ceram. Soc. 2–3 (2007) 1273–1279.
[46] E. Rocha-Rangel, J.G. Miranda-Hernández, S. Moreno-Guerrero, A.B. Soto-Guzmán, J. Ceram. Process. Res. 7 (2006) 311–314.
[47] M. Lieberthal, W.D. Kaplan, Mater. Sci. Eng., A 302 (2001) 83–91.
[48] E. Lucchini, S. Lo Casto, O. Sbaizero, Mater. Sci. Eng. 357 (2003) 369–375.
[49] N. Travitzky, I. Gotman, N. Claussen, Mater. Lett. 57 (2003) 3422–3426.
[50] V.M. Sglavo, F. Marino, B.R. Zhang, S. Gialanella, Mater. Sci. Eng., A 239–240 (1997) 665–671.
[51] J.G. Miranda-Hernández, S. Díaz de la Torre, E. Rocha-Rangel, Epit. J. Silic. Bas. Comp. Mater. 62 (2010) 2–5.
[52] P. Auerkari, Mechanical and Physical Properties of Engineering Alumina Ceramics, Technical Research Centre of Finland: Espoo, Finland, 1996, p. 23.